Contents

Governing equations

Fluid-structure interaction (FSI) combines two classical fields of mechanics, computational fluid mechanics (CFD), and computational structural mechanics (CSM). To complete FSI there is also the coupling, or interaction between these two. A separate understanding of the fluid and structure is therefore necessary to understand the full problem. This chapter presents the governing equations of the individual fluid and structure problem. Balance laws together with auxiliary kinematic, dynamic, and material relations will be described briefly.

1.1 Continuum Mechanics

In our effort to understand and describe physical phenomenon in nature, we describe our observations and theories by creating mathematical models. The mathematical models makes scientist and engineers not only able to understand physical phenomena, but also predict them. All matter is built up by a sequence of atoms, meaning on a microscopic level, an observer will locate discontinuties and space within the material. Evaluating each atom, or *material point*, is not impossible from a mathematical point of view. However, for mathematical moddeling and applications, the evaluation of each material point remains unpractical. In *continuum mechanics*, first formulated by Augustin-Louis Cauchy [23], the microscopic structure of materials are ignored, assuming the material of interest is *continuously distributed* in space, referred to as a continuum.

In context of this thesis we define a *continuum* as a continuous body $V(t) \subset \mathbb{R}^d$ $d \in (1, 2, 3)$, continuously distributed throughout its own extension. The continuum is assumed to be infinitely divisible, meaning one can divide some region of the continuum a indefinitely number of times. A continuum is also assumed to be locally homogeneous, meaning if a continuum is subdivided into infinitesimal regions, they would all have the same properties such as mass density. These two properties forms the baseline for deriving conservation laws and constitute equations, which are essential for formulating mathematical models for both CFD and CSM. However, a continuum remains a mathematical idealization, and may not be a reasonable model for certain applications. In general, continuum mechanics have proven to be applicable provided that $\frac{\delta}{l} << 1$ where δ is a characteristic length scale of the material micro-structure, and l is a length scale of the problem of interest [19].

1.2 The Lagrangian and Eulerian description of motion

In continuum mechanics, one makes use if two classical description of motion, the *Lagrangian* and *Eulerian* description. Both concepts are related to an observers view of motion, visually explained by the concepts of *material* and *spatial* points. A material points represents a particle within the material, moving with the material as it move and deform. A spatial point, refers to some reference at which the path of the material points are measured from.

Lagrangian

In the Lagrangian description of motion, the material and spatial points coincide, meaning the reference point of which motion is measured, follows the material as it diverts from its initial position. The initial position of all material points in a continuum extend a region, called the *reference configuration* $\hat{V}$. From now on, all identities in the *reference configuration* will be denoted with the notation "$\wedge$". If a continuum deviates from its reference configuration, a material point $\hat{\mathbf{x}}(x, y, z, t)$ may no longer be at its initial position, but moved to a new position $\mathbf{x}(x, y, z, t)$ at time t. The new positions of all material points extend a new region, called the *current configuration* $V(t)$.

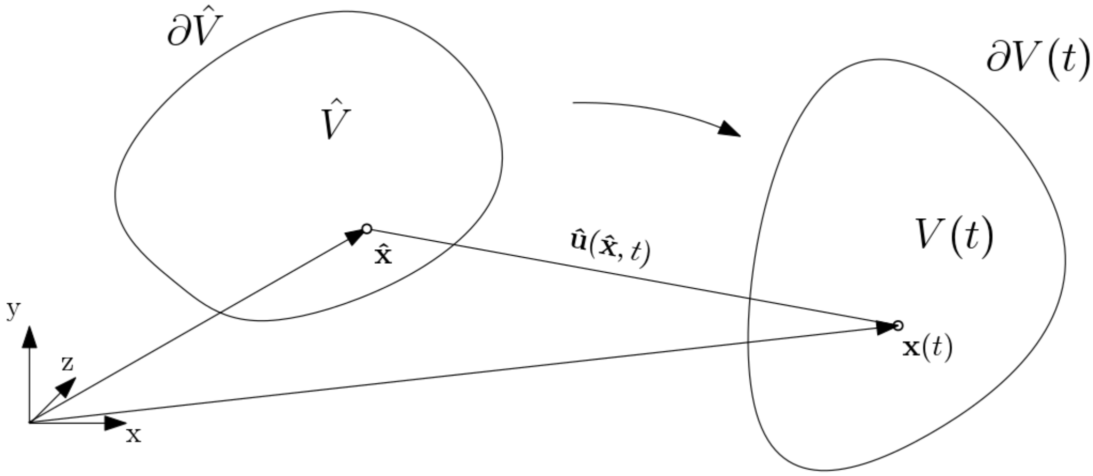

Figure 1.1: A visual representation of the Lagrangian description of motion.

To measure the displacement of a material point $\mathbf{x} \in V(t)$ for time t, from its initial point $\hat{\mathbf{x}} \in \hat{V}$, one defines a *deformation vector field*

$$\hat{\mathbf{u}}(\hat{\mathrm{x}}, t) = x(\hat{\mathbf{x}}, t) - \hat{\mathbf{x}} = \hat{\mathrm{T}}(\hat{\mathbf{x}}, t) \tag{1.1}$$

Mathematically, deformation is a 1:1 mapping $\hat{\mathrm{T}}(\hat{\mathbf{x}}, t)$, transforming material points from the *reference configuration* $\hat{V}$, to the *current configuration* $V(t)$. Visually, the deformation resembles the shape of continuum for some time t. To describe the continuums motion, one defines the *velocity vector field* given by the time derivative of the deformation field,

$$\hat{\mathbf{v}}(\hat{\mathrm{x}}, t) = d_t x(\hat{\mathbf{x}}, t) = d_t \hat{\mathbf{u}}(\hat{\mathbf{x}}, t) = \frac{\partial \hat{\mathrm{T}}(\hat{\mathrm{x}}, t)}{\partial t} \tag{1.2}$$

The Lagrangian description of motion is the natural choice when tracking particles and surfaces are of main interest. Therefore, it is mainly used within structure mechanics.

Eulerian

In the Eulerian description of motion, the material and spatial points are separated. Instead of tracking material points $\hat{x}(t) \in V(t)$, the attention brought to a fixed view-point V. In contrary with the Lagrangian description, the *current configuration* is chosen as the *reference configuration*, not the initial position of all material particles. The location or velocity of any material particle is not of interest, but rather the properties of a material particle happening to be at $\mathbf{x}(t)$ for some t.

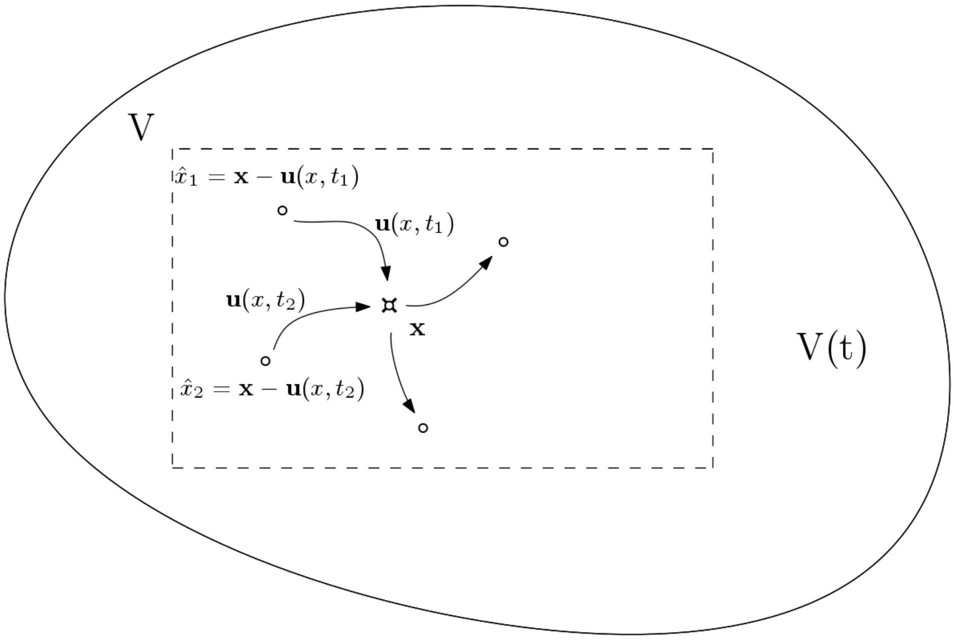

Figure 1.2: A visual representation of the Eulerian description of motion. For a view-point V fixed in time, a spatial coordinate $\mathbf{x}$ measures properties of a material particle $\hat{x}$ from the moving continuum $V(t)$.

We can describe the particles occupying the *current configuration* $V(t)$ for some time $t \geq t_0$

$$\mathbf{x} = \hat{\mathbf{x}} + \hat{\mathbf{u}}(\hat{\mathrm{x}}, t)$$

Since our domain is fixed we can define the deformation for a particle occupying position $x = x(\hat{\mathrm{x}}, t)$ as

$$\mathbf{u}(x, t) = \hat{\mathbf{u}}(\hat{\mathbf{x}}, t) = x - \hat{\mathbf{x}}$$

and its velocity

$$\mathbf{v}(\hat{\mathbf{x}}, t) = \partial_t \mathbf{u}(\hat{\mathbf{x}}, t) = \partial_t \hat{\mathbf{u}}(\hat{\mathbf{x}}, t) = \hat{\mathbf{v}}(\hat{\mathbf{x}}, t)$$

The Eulerian description falls naturally for describing fluid flow, due to local kinematic properties are of higher interest rather than the shape of fluid domain. Using a Lagrangian description for fluid flow would also be tidious, due to the large number of material particles appearing for longer simulations of fluid flow. A comparison of the two previous mentioned description is shown of In Figure 1.3.

1.3 The Solid problem

The solid governing equations is given by,

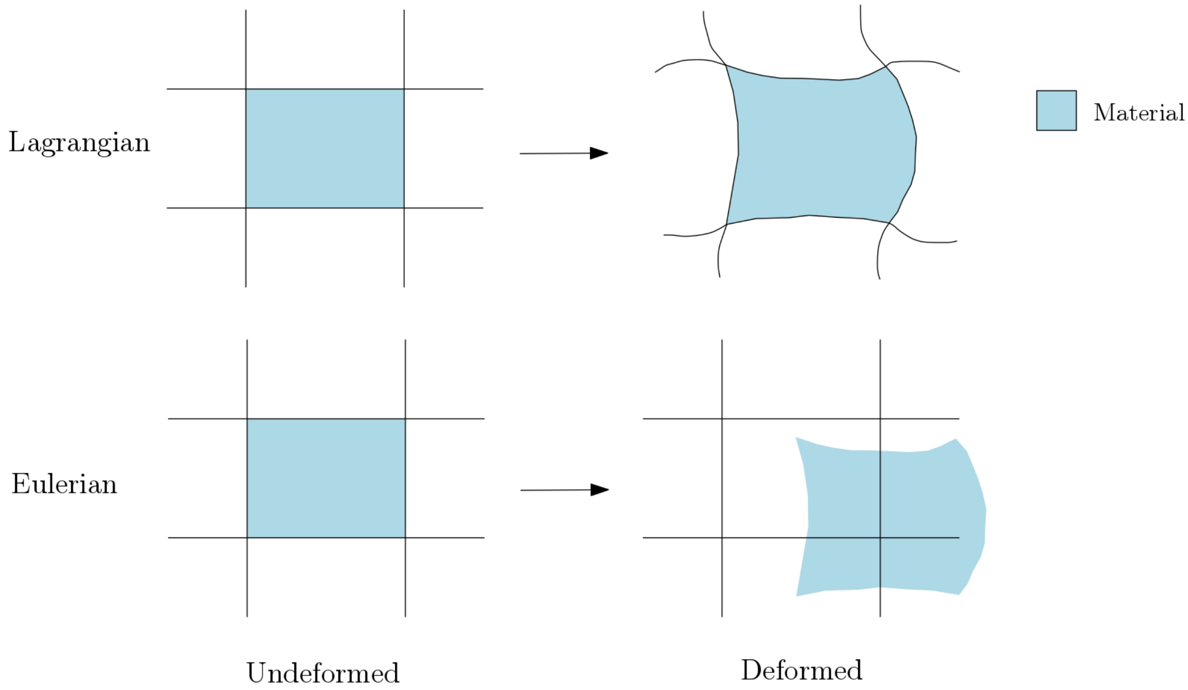

Figure 1.3: Comparison of the Lagrangian and Eulerian description of motion.

Equation 1.3.1. *Solid momentum*

$$\rho_s \frac{\partial \hat{\mathbf{v}}_s}{\partial t} = \nabla \cdot (\hat{J}\sigma_s \hat{\mathbf{F}}^{-T}) + \rho_s \mathbf{f}_s \quad \text{in } \hat{\Omega}_s \tag{1.3}$$

$$\frac{\partial \hat{\mathbf{v}}_s}{\partial t} = \hat{\mathbf{u}}_\mathbf{s} \quad \text{in } \hat{\Omega}_s \tag{1.4}$$

defined in a Lagrangian coordinate system, with respect to an initial reference configuration $\hat{\Omega}_s$. The structure configuration is given by the displacement $\hat{\mathbf{u}}_s$, with the relation $\frac{\partial \hat{\mathbf{v}}}{\partial t} = \hat{\mathbf{u}}_s$ to the solid velocity. The density of the structure is given by ρ_s, and $\hat{\mathbf{f}}_s$ express any exterior body forces acting. Finally, $\hat{\mathbf{F}} = I + \nabla\hat{\mathbf{u}}_s$ is the deformation gradient, and $\hat{J}$ is the determinant of $\hat{\mathbf{F}}$ *(See Appendix* **??** *for further detail).*

Material models express the dependency between strain tensors and stress. The validity of material models is often limited by their ability to handle deformation and strain to some extent, before it breaks down or yields nonphysical observations of the material. In this thesis, we assume a linear relation between stress and strain, where the elasticity of the material is expressed by the *Poisson ratio* ν_s, *Young modulus* E, or Lamè coefficients λ_s and μ_s. Their relation is given by,

$$E_y = \frac{\mu_s(\lambda_s + 2\mu_s)}{(\lambda_s + \mu_s)} \qquad \nu_s = \frac{\lambda_s}{2(\lambda_s + \mu_s)}$$

$$\lambda_s = \frac{\nu E_y}{(1+\nu_s)(1-2\nu_s)} \qquad \mu_s = \frac{E_y}{2(1+\nu_s)}$$

The first order *Hooke´s law*, is applicable for small-scale deformations,

Definition 1.1. Let $\hat{u}$ be a differential deformation field in the *reference* configuration, I be the Identity matrix, and the gradient $\hat{\nabla} = (\frac{\partial}{\partial x}, \frac{\partial}{\partial y}, \frac{\partial}{\partial z})$. *Hooke's law* is then given by,

$$\sigma_s = \frac{1}{\hat{J}}\hat{\mathbf{F}}(\lambda_s(Tr(\epsilon)I + 2\mu\epsilon)\hat{\mathbf{F}}$$
$$\hat{\mathbf{S}}_s = \lambda_s(Tr(\epsilon)I + 2\mu\epsilon$$
$$\epsilon = \frac{1}{2}(\hat{\nabla}\hat{\mathbf{u}} + (\hat{\nabla}\hat{\mathbf{u}})^T)$$

Hooke's law is however limited to a small-deformation regime, and fails for larger deformations encountered in this thesis. A valid model for larger deformations is the hyper-elastic *St. Vernant-Kirchhoff model*(STVK), extending Hooke's law into a non-linear regime.

Definition 1.2. Let $\hat{u}$ be a differential deformation field in the *reference* configuration, I be the Identity matrix and the gradient $\hat{\nabla} = (\frac{\partial}{\partial x}, \frac{\partial}{\partial y}, \frac{\partial}{\partial z})$. The *St. Vernant-Kirchhoff model* is then given by the relation,

$$\sigma_s = \frac{1}{\hat{J}}\hat{\mathbf{F}}(\lambda_s(Tr(\hat{\mathbf{E}})I + 2\mu\hat{\mathbf{E}})\hat{\mathbf{F}}^{-T}$$
$$\hat{\mathbf{S}}_s = \lambda_s(Tr(\hat{\mathbf{E}})I + 2\mu\hat{\mathbf{E}}$$
$$\hat{\mathbf{E}} = \frac{1}{2}(\hat{\mathbf{C}} - I) \quad \hat{\mathbf{C}} = \hat{\mathbf{F}}\hat{\mathbf{F}}^{-T}$$

where $\hat{\mathbf{C}}$ *is the right Cauchy-Green strain tensor and* $\hat{\mathbf{E}}$ *is the Green Lagrangian strain tensor (See appendix B for definition)*

Though STVK can handle large deformations, it is not valid for large strain [27]. However since the strain considered in this thesis are small, it will remain our primary choice of strain-stress relation.
In addition, initial condition and boundary condition is supplemented for the problem to be well posed. The first type of of boundary conditions are Dirichlet boundary conditions,

$$\mathbf{v}_s = \mathbf{v}_s^D \quad \text{on } \Gamma_s^D \subset \partial\Omega_s \tag{1.5}$$
$$\mathbf{d}_s = \mathbf{d}_s^D \quad \text{on } \Gamma_s^D \subset \partial\Omega_s \tag{1.6}$$
$$\tag{1.7}$$

The second type of boundary condition are Neumann boundary conditions

$$\sigma_s \cdot \mathbf{n} = \mathbf{g} \quad \text{on } \Gamma_s^N \subset \partial\Omega_s \tag{1.8}$$

1.4 The Fluid problem

The fluid is assumed to be express by the in compressible Navier-Stokes equations,

Equation 1.4.1. *Navier-Stokes equation*

$$\rho\frac{\partial \mathbf{v}_f}{\partial t} + \rho\mathbf{v}_f \cdot \nabla\mathbf{v}_f = \nabla \cdot \sigma + \rho\mathbf{f}_f \quad \text{in } \Omega_f \tag{1.9}$$

$$\nabla \cdot \mathbf{v}_f = 0 \quad \text{in } \Omega_f \tag{1.10}$$

defined in an Eulerian description of motion. The fluid density as ρ_f and fluid viscosity ν_f are assumed to be constant in time, and $\mathbf{f}_s$ represents any body force. The fluid is assumed Newtonian, where *Cauchy stress sensor* follows Hooke's law

$$\sigma = -p_f I + \mu_f(\nabla\mathbf{v}_f + (\nabla\mathbf{v}_f)^T$$

As for the solid problem, boundary conditions are supplemented considering Dirichlet boundary conditions,

$$\mathbf{v}_f = \mathbf{v}_f^D \quad \text{on } \Gamma_v^D \subset \partial\Omega_f \tag{1.11}$$

$$p_f = p_f^D \quad \text{on } \Gamma_p^D \subset \partial\Omega_f \tag{1.12}$$

The second type of boundary condition are Neumann boundary conditions

$$\sigma_f \cdot \mathbf{n} = \mathbf{g} \quad \text{on } \Gamma_f^N \subset \partial\Omega_f \tag{1.13}$$

Appendices

The deformation gradient

?? Deformation is a major property of interest when a continuum is influenced by external and internal forces. The deformation results in relative change of position of material particles, called *strain*. and is the primary property that causes and describe *stress*. Strain is purely an observation, and it is not dependent on the material of interest. However one expects that a material undergoing strain, will give forces within a continuum due to neighboring material particles interacting with one another. Therefore one derive material specific models to describe how a certain material will react to a certain amount of strain. These strain measures are used to define models for *stress*, which is responsible for the deformation in materials [15]. Stress is defined as the internal forces that particles within a continuous material exert on each other, with dimension force per unit area.

The equations of continuum mechanics can be derived with respect to either a deformed or undeformend configuration. The choice of refering our equations to the current or reference configuration is indifferent from a theoretical point of view. In practice however this choice can have a severe impact on our strategy of solution methods and physical of modelling. [54]. Regardless of configuration, the *deformation gradient* and *determinant of the deformation gradient* are essential measurement in structure mechanics. By [29], both configurations are considered.

Reference configuration

Definition A.1. Let $\hat{u}$ be a differential deformation field in the *reference* configuration, I be the Identity matrix and the gradient $\hat{\nabla} = (\frac{\partial}{\partial x}, \frac{\partial}{\partial y}, \frac{\partial}{\partial z})$. Then the *deformation gradient* is given by,

$$\hat{\mathbf{F}} = I + \hat{\nabla}\hat{\mathbf{u}} \tag{A.1}$$

expressing the local change of relative position under deformation.

Definition A.2. Let $\hat{u}$ be a differential deformation field in the *reference* configuration, I be the Identity matrix and the gradient $\hat{\nabla} = (\frac{\partial}{\partial x}, \frac{\partial}{\partial y}, \frac{\partial}{\partial z})$. Then the *determinant of the deformation gradient* is given by,

$$J = det(\hat{\mathbf{F}}) = det(I + \hat{\nabla}\hat{\mathbf{u}}) \tag{A.2}$$

expressing the local change of volume the configuration.

From the assumption of linear operator $\mathbf{F}$, and no two particles $\hat{\mathbf{x}}_a, \hat{\mathbf{x}}_b \in \hat{\mathrm{V}}$ occupy the same location for some time $V(t)$, J to be greater than 0 [54].

Current configuration

Definition A.3. Let $\mathbf{u}$ be a differential deformation field in the *reference* configuration, I be the Identity matrix and the gradient $\nabla = (\frac{\partial}{\partial x}, \frac{\partial}{\partial y}, \frac{\partial}{\partial z})$. Then the *deformation gradient* is given by,

$$\mathbf{F} = I - \nabla \mathbf{u} \tag{A.3}$$

expressing the local change of relative position under deformation.

Definition A.4. Let $\mathbf{u}$ be a differential deformation field in the *reference* configuration, I be the Identity matrix and the gradient $\nabla = (\frac{\partial}{\partial x}, \frac{\partial}{\partial y}, \frac{\partial}{\partial z})$. Then the *determinant of the deformation gradient* is given by,

$$J = det(\mathbf{F}) = det(I - \nabla \mathbf{u}) \tag{A.4}$$

expressing the local change of volume the configuration.

Strain tensor

?? The equations describing forces on our domain can be derived in accordinance with the current or reference configuration. With this in mind, different measures of strain can be derived with respect to which configuration we are interested in. We will here by [29] show the most common measures of strain. We will first introduce the right *Cauchy-Green* tensor $\mathbf{C}$, which is one of the most used strain measures [54].
Uttrykk 1.3 fra Godboka, LAG TEGNING

Let $\hat{\mathrm{x}}, \hat{\mathrm{y}} \in \hat{\mathrm{V}}$ be two points in our referemce configuration and let $\hat{\mathrm{a}} = \hat{\mathrm{y}} - \hat{\mathrm{x}}$ denote the length of the line bewtween these two points. As our domain undergoes deformation let $x = \hat{\mathrm{x}} + \hat{u}(\hat{\mathrm{x}})$ and $x = \hat{\mathrm{y}} + \hat{u}(\hat{\mathrm{y}})$ be the position of our points in the current configuration, and let $a = y - x$ be our new line segment. By [29] we have by first order Taylor expansion

$$
\begin{aligned}
&y - x = \hat{\mathrm{y}} + \hat{u}(\hat{\mathrm{y}}) - \hat{\mathrm{x}} - \hat{u}(\hat{\mathrm{x}}) = \ \hat{\mathrm{y}} - \hat{\mathrm{x}} + \hat{\nabla}\hat{\mathrm{u}}(\hat{\mathrm{x}})(\hat{\mathrm{y}} - \hat{\mathrm{x}}) + \mathcal{O}(|\hat{\mathrm{y}} - \hat{\mathrm{x}}|^2) \\
&\frac{y - x}{|\hat{\mathrm{y}} - \hat{\mathrm{x}}|} = [I + \hat{\nabla}\hat{u}(\hat{\mathrm{x}}]\frac{\hat{\mathrm{y}} - \hat{\mathrm{x}}}{|\hat{\mathrm{y}} - \hat{\mathrm{x}}|} + \mathcal{O}(|\hat{\mathrm{y}} - \hat{\mathrm{x}}|)
\end{aligned}
$$

This detour from [29] we have that

$$
\begin{aligned}
&a = y - x = \hat{F}(\hat{\mathrm{x}})\hat{\mathrm{a}} + \mathcal{O}(|\hat{\mathrm{a}}|^2) \\
&|a| = \sqrt{(\hat{F}\hat{\mathrm{a}}, \hat{F}\hat{\mathrm{a}}) + \mathcal{O}(|\hat{\mathrm{a}}^3|)} = \sqrt{(\hat{\mathrm{a}}^T, \hat{F}^T\hat{F}\hat{\mathrm{a}})} + \mathcal{O}(|\hat{\mathrm{a}}^2|)
\end{aligned}
$$

We let $\hat{\mathrm{C}} = \hat{\mathrm{F}}^T\hat{\mathrm{F}}$ denote the right *Cauchy-Green tensor*. By observation the Cauchy-Green tensor is not zero at the reference configuration

$$
\hat{\mathrm{C}} = \hat{\mathrm{F}}^T\hat{\mathrm{F}} = (I + \hat{\nabla}\hat{\mathrm{u}})^T(I + \hat{\nabla}\hat{\mathrm{u}}) = 1
$$

Hence it is convenient to introduce a tensor which is zero at the reference configuration. We define the *Grenn-Lagrange strain tensor*, which arises from the squard rate of change of the linesegment $\hat{\mathrm{a}}$ and a. By using the definition of the Cauchy-Green tensor we have the relation

$$
\begin{aligned}
&\frac{1}{2}(|a|^2 + |\hat{\mathrm{a}}|^2) = \frac{1}{2}(\hat{\mathrm{a}}^T\hat{C}\hat{\mathrm{a}} - \hat{\mathrm{a}}^T\hat{\mathrm{a}}) + \mathcal{O}(|\hat{\mathrm{a}}^3| = \hat{\mathrm{a}}^T\big(\frac{1}{2}(\hat{F}^T\hat{F} - I)\big)\hat{\mathrm{a}} + \mathcal{O}(\hat{\mathrm{a}}^3) \\
&\hat{E} = \frac{1}{2}(\hat{C} - I)
\end{aligned}
$$

Both the *right Cauchy-Green tensor* $\hat{C}$ and the *Green-Lagrange* $\hat{E}$ are refered to the Lagrangian coordinate system, hence the *reference configuration.*
Using similar arguments (see [29], compsda) Eulerian counterparts of the Lagrangian stress tensors can be derived.
The *left Cauchy-Green* strain tensor

$$\mathbf{b} = \hat{\mathrm{F}}\hat{\mathrm{F}}^T =$$

and the *Euler-Almansi* strain tensor

$$\mathbf{e} = \frac{1}{2}(I - \hat{F}^{-1}\hat{F}^{-T}) = \hat{F}^{-1}\hat{E}\hat{F}^T$$

Bibliography

[1] Martin Alnæs, Anders Logg, Kristian Ølgaard, Marie Rognes, and Garth Wells. Unified Form Language: A domain-specific language for weak formulations of partial differential equations. *IJCAI International Joint Conference on Artificial Intelligence*, 2015-Janua(212):4207–4211, 2015.

[2] Robert T Biedron and Elizabeth M Lee-Rausch. Rotor Airloads Prediction Using Unstructured Meshes and Loose CFD/CSD Coupling.

[3] P I Crumpton. Implicit time accurate solutions on unstructured dynamic grids. (95):1–23, 1995.

[4] J Donea, A Huerta, J.-Ph Ponthot, and A Rodríguez-Ferran. Arbitrary Lagrangian-Eulerian methods. (1969):1–38, 2004.

[5] Richard P Dwight. Robust Mesh Deformation using the Linear Elasticity Equations.

[6] Stéphane Étienne, D Tremblay, and Dominique Pelletier. Code Verification and the Method of Manufactured Solutions for Fluid-Structure Interaction Problems. *36th AIAA Fluid Dynamics Conference and Exhibit*, (June):1–11, 2006.

[7] Miguel A Fernández and Jean-Frédéric Gerbeau. Algorithms for fluid-structure interaction problems. 2009.

[8] Miguel A. Fernández, Jean Frederic Gerbeau, and Ceremade Grandmont. A projection semi-implicit scheme for the coupling of an elastic structure with an incompressible fluid. *International Journal for Numerical Methods in Engineering*, 69(4):794–821, 2007.

[9] L Formaggia and F Nobile. A stability analysis for the arbitrary Lagrangian Eulerian formulation with finite elements. *East-west journal of numerical mathematics*, Vol. 7(No. 2):105–131, 1991.

[10] Luca Formaggia and Fabio Nobile. Stability analysis of second-order time accurate schemes for ALE-FEM. *Computer Methods in Applied Mechanics and Engineering*, 193(39-41 SPEC. ISS.):4097–4116, 2004.

[11] Christiane Förster, Wolfgang A. Wall, and Ekkehard Ramm. Artificial added mass instabilities in sequential staggered coupling of nonlinear structures and incompressible viscous flows. *Computer Methods in Applied Mechanics and Engineering*, 196(7):1278–1293, 2007.

[12] Bernhard Gatzhammer. Efficient and Flexible Partitioned Simulation of Fluid-Structure Interactions. page 261, 2014.

[13] Philippe Geuzaine. Numerical Simulations of Fluid-Structure Interaction Problems using MpCCI. (1):1–5.

[14] Brian T. Helenbrook. Mesh deformation using the biharmonic operator. *International Journal for Numerical Methods in Engineering*, 2003.

[15] Gerhard A. Holzapfel. *Nonlinear Solid Mechanics: A Continuum Approach for Engineering*. 2000.

[16] Jaroslav Hron and Stefan Turek. Proposal for numerical benchmarking of fluid-structure interaction between an elastic object and laminar incompressible flow. *Fluid-Structure Interaction*, 53:371–385, 2006.

[17] Ming-Chen Hsu and Yuri Bazilevs. Fluid–structure interaction modeling of wind turbines: simulating the full machine. *Computational Mechanics*, 50(6):821–833, dec 2012.

[18] Su-Yuen Hsu, Chau-Lyan Chang, and Jamshid Samareh. A Simplified Mesh Deformation Method Using Commercial Structural Analysis Software.

[19] Jay D. Humphrey. *Cardiovascular Solid Mechanics*. Springer New York, New York, NY, 2002.

[20] Hrvoje Jasak and Željko Tuković. Automatic mesh motion for the unstructured Finite Volume Method. *Transactions of Famena*, 30(2):1–20, 2006.

[21] Jae-Hyun Kim and Hyung-Cheol Shin. Application of the ALE technique for underwater explosion analysis of a submarine liquefied oxygen tank. *Ocean Engineering*, 35(8-9):812–822, jun 2008.

[22] V V Meleshko. Bending of an Elastic Rectangular Clamped Plate: Exact Versus 'Engineering' Solutions. *Journal of Elasticity*, 48(1):1–50, 1997.

[23] José Merodio and Giuseppe Saccomandi. Continuum Mechanics - Volume I. In *Volume 1*, chapter 3, pages 82–84. EOLSS, 2011.

[24] Selim MM and Koomullil RP. Mesh Deformation Approaches – A Survey. *Journal of Physical Mathematics*, 7(2), 2016.

[25] J Newman. *Marine Hydrodynamics*. 1977.

[26] William L. Oberkampf and Christopher J. Roy. *Verification and Validation in Scientific Computing*. Cambridge University Press, Cambridge, 2010.

[27] M Razzaq, Stefan Turek, Jaroslav Hron, J F Acker, F Weichert, I Grunwald, C Roth, M Wagner, and B Romeike. Numerical simulation and benchmarking of fluid-structure interaction with application to Hemodynamics. *Fundamental Trends in Fluid-Structure Interaction*, 1:171–199, 2010.

[28] T. Richter and T. Wick. Finite elements for fluid-structure interaction in ALE and fully Eulerian coordinates. *Computer Methods in Applied Mechanics and Engineering*, 199(41-44):2633–2642, 2010.

[29] Thomas Richter. Fluid Structure Interactions. 2016.

[30] Thomas Richter and Thomas Wick. On Time Discretizations of Fluid-Structure Interactions. pages 377–400. 2015.

[31] Patrick J. Roache. Code Verification by the Method of Manufactured Solutions. *Journal of Fluids Engineering*, 124(1):4, 2002.

[32] P.J. Roache. *Verification and Validation in Computational Science and Engineering*. Computing in Science Engineering, Hermosa Publishers, 1998, 8-9, 1998.

[33] Edward J. Rykiel. Testing ecological models: The meaning of validation. *Ecological Modelling*, 90(3):229–244, 1996.

[34] Kambiz Salari and Patrick Knupp. Code Verification by the Method of Manufactured Solution. Technical report, Sandia National Laboratories, 2000.

[35] LE Schwer. Guide for verification and validation in computational solid mechanics. *American Society of Mechanical Engineers*, PTC 60(V&V 10):1–15, 2006.

[36] Jason P Sheldon, Scott T Miller, and Jonathan S Pitt. Methodology for Comparing Coupling Algorithms for Fluid-Structure Interaction Problems. *World Journal of Mechanics*, 4(February):54–70, 2014.

[37] J.C. Simo and F. Armero. Unconditional stability and long-term behavior of transient algorithms for the incompressible Navier-Stokes and Euler equations. *Computer Methods in Applied Mechanics and Engineering*, 111(1-2):111–154, jan 1994.

[38] Ian Sommerville. Verification and Validation. Technical Report February, 2006.

[39] K Stein, T Tezduyar, and R Benney. Mesh Moving Techniques for Fluid-Structure Interactions With Large Displacements.

[40] Keith Stein, Richard Benney, Tayfun Tezduyar, and Jean Potvin. Fluid–structure interactions of a cross parachute: numerical simulation. *Computer Methods in Applied Mechanics and Engineering*, 191(6-7):673–687, dec 2001.

[41] Ryo Torii, Marie Oshima, Toshio Kobayashi, Kiyoshi Takagi, and Tayfun E. Tezduyar. Fluid–structure interaction modeling of a patient-specific cerebral aneurysm: influence of structural modeling. *Computational Mechanics*, 43(1):151–159, dec 2008.

[42] Stefan Turek, Jaroslav Hron, Mudassar Razzaq, and Hilmar Wobker. Numerical Benchmarking of Fluid-Structure Interaction : A comparison of different discretization and solution approaches.

[43] A V, T Passerini, A Quaini, U Villa, A Veneziani, and S Canic. Numerical Analysis and S cientific C omputing P reprint S eria Validation of an open source framework for the simulation of blood flow in rigid and deformable vessels P reprint # 17 D epartment of Mathematics University of Houston. 2013.

[44] Jan Vierendeels. Comparison of the Hemodynamic and Thrombogenic Performance of Two Bileaflet Mechanical Heart Valves Using a CFD/FSI Model. *Journal of Biomechanical Engineering*, 129(4):558, jan 2007.

[45] Wolfgang A. Wall, Axel , Gerstenberger, Peter , Gamnitzer, Christiane , Förster, and Ekkehard , Ramm. Large Deformation Fluid-Structure Interaction – Advances in ALE Methods and New Fixed Grid Approaches. In *Fluid-Structure Interaction: Modelling, Simulation, Optimisation*, pages 195—-232. Springer Berlin Heidelberg, 2006.

[46] Frank White. *Viscous fluid flow*. McGraw-Hill, third edit edition.

[47] T. Wick. Stability Estimates and Numerical Comparison of Second Order Time-Stepping Schemes for Fluid-Structure Interactions. In *Numerical Mathematics and Advanced Applications 2011*, pages 625–632. Springer Berlin Heidelberg, Berlin, Heidelberg, 2013.

[48] T Wick and Thomas Wick. Variational-monolithic ALE fluid-structure interaction: Comparison of computational cost and mesh regularity using different mesh motion techniques.

[49] Thomas Wick. *Adaptive Finite Element Simulation of Fluid-Structure Interaction with Application to Heart-Valve*. PhD thesis, Heidelberg.

[50] Thomas Wick. Solving Monolithic Fluid-Structure Interaction Problems in Arbitrary Lagrangian Eulerian Coordinates with the deal.II Library.

[51] Thomas Wick. Fluid-structure interactions using different mesh motion techniques. *Computers and Structures*, 89(13-14):1456–1467, 2011.

[52] Thomas Wick. Fully Eulerian fluid-structure interaction for time-dependent problems. *Computer Methods in Applied Mechanics and Engineering*, 255:14–26, 2013.

[53] Klaus Wolf, Schloss Birlinghoven, Code Coupling Interface, Open Programming Interface, and Distributed Simulation. Mpcci – the Generl Code Coupling Interface. *6. LS-DYNA Anwenderforum, Frankenthal 2007 IT*, pages 1–8, 2007.

[54] P. Wriggers. *Computational contact mechanics, second ed., Springer*. 2006.

[55] Hou Zhang, Xiaoli Zhang, Shanhong Ji, Yanhu Guo, Gustavo Ledezma, Nagi Elabbasi, and Hugues DeCougny. Recent development of fluid-structure interaction capabilities in the ADINA system. *Computers and Structures*, 81(8-11):1071–1085, 2003.